INVESTIGATION ON THE ENHANCEMENT OF HEAT TRANSFER IN COUNTERFLOW DOUBLE-PIPE HEAT EXCHANGER USING NANOFLUIDS

by

Varadhan BALAN [a*], Surendran RAMAKRISHNAN [b], Gopinath PALANI [b], and Mayakannan SELVARAJU [c]

[a] Department of Mechanical Engineering, KSR College of Engineering, Tiruchengode, Namakkal, Tamilnadu, India
[b] Department of Mechanical Engineering, KSR Institute for Engineering and Technology, Tiruchengode, Namakkal, Tamilnad, India
[c] Department of Mechanical Engineering, Vidyaa Vikas College of Engineering and Technology, Tiruchengode, Namakkal, Tamilnadu, India

Original scientific paper
https://doi.org/10.2298/TSCI230312273V

Particles less than 100 nanometers in size are suspended in a base fluid such as water, oil, and ethylene glycol. These nanoparticles are floating in the nanofluid. The purpose of this study is to research the operation of a counter-flowing, double-pipe heat exchanger using two distinct nanofluids as cooling media. Titanium carbide and carbon nanotubes combine to form alkaline water, a basic fluid. The purpose of this research was to assess the performance of a counterflow double-pipe heat exchanger using water with different concentrations of titanium carbide and carbon nanotubes. Alkaline water had a particle volume concentration of 0.06, and its nanofluid-flow rate was 0.03. Using a heat exchanger, water is heated to 65 °C while nanofluids are heated to 35 °C, both at a constant input velocity. The speed of both fluids is constant. The findings demonstrate that nanofluid outperforms water in heat absorption across a broad range of flow speeds. Heat exchangers benefit from the improved thermal characteristics of nanoscale fluids.

Key words: *heat exchange, titanium carbide, carbon nanotubes, nanofluid, velocity*

Introduction

Scientists have developed a wide variety of heat transfer systems in an effort to rise the dependability of the various existing heat transfer technologies. The larger of the two tubes does all of the work of heat transfer [1]. The internal pipe prevents electricity from escaping through the outer pipe by acting as a conductive barrier. The time it takes for fluid to move from the pipe wall or anywhere else internal pipe to the outlet rises when there are obstructions in the pipe. It is possible to increase the liquid's heat conduction rate by adding chemicals to the mixture. There are several ways to accomplish this, and this is one of them. Increasing the thermal conductivity of a fluid has many benefits, one of which is a marked improvement in the medium's capacity for transporting and dissipating heat [2]. The high thermal conductivity of these materials greatly benefits heat transfer since it enables the heat transfer fluid to quickly

* Corresponding author, e-mail: uvbalan@gmail.com

and efficiently warm the target surface. Studies undertaken over the past few years have shown that traditional fluids are not as effective as nanofluids at transmitting heat. The breakthrough was found by contrasting the two fluids under study. Mechanical systems frequently use heat transfer fluids including water, propylene glycol, countless, and ethylene glycol more to keep things at a comfortable temperature [3]. Fluids employed for one purpose of heat transfer typically find additional uses. However, these more prevalent fluids have a limited capacity for heat transfer. Unique fluids utilised for thermal transfer are collectively mentioned as *nanofluids*, a term used to define this class of materials [4, 5]. To achieve this, he mixed fundamental fluids with particles having a diameter of 1100 nm.

Many scientific journals feature experiments that investigate what happens when nanofluids are introduced to channels with varying flow morphology. The purpose of these research's was to obtain evidence. The primary motivation for this study was to learn more about what affects heat transfer rates and why. Using a circumferential tube and a static shearing temperature and an incompressible viscous transfer of heat rate, we studied the impacts of nanoparticles of metal oxide dispersing in a fluid. Scientists proved the usefulness of Al_2O_3-water nanofluids by expanding the flow area of a tube with a constant heat flux [6]. This was discovered utilizing computational simulations of laminar circulation in a channel of rectangle by examining the heat transfer characteristics along the continuous flux of heat experienced by the enhanced flow zone of the tube [7, 8]. In their study, the scientists take into consideration the nanofluids' heat transmission and frictional resistance. Al_2O_3, Cu, and SiO_2 nanoparticles were investigated for their potential to enhance heat conduction in a variety of settings.

While keeping the nanoparticles' 25 nm diameter constant, researchers shifted the volume fractions from 0.5-2.5%. Researchers in a study published in *Nature Communications* looked at the boil rate of heat transmission in a line of communication using alkaline drinking water and nanofluids. The studies show that the nanofluid can transmit heat more efficiently than water. In order to evaluate the duct's efficacy, scientists pumped laminar CuO-water nanofluid through it, subjecting it to a constant heat flux. This allowed them to assess the duct's efficiency [9]. The coefficient of heat transfer of the CuO-water nanofluid was found to be greater than that of regular tap water. The authors performed controlled temperature testing of three non-Newtonian nanofluids in a circular tube. All of these nanofluids contained oxides, including TiO_2, Al_2O_3, and CuO. The convective heat transfer rate of nanodispersions including nanoparticles was found to be greater than that of the base fluid [10].

The coefficient of heat transfer between water and lignite nanofluids was determined using their respective convective thermal conductivities. We did this because it was suggested by the writers. The TiO_2-water nanoparticles' thermal and rheological properties were investigated with the use of the DPHE [11]. Several adjustments, including the addition of nanoparticles, were performed to the heat exchanger to accomplish this goal. The authors conducted additional research to determine the extent of heat transmission from the TiO_2-water nanofluid to the water within the heat exchanger. More studies were done to quantify the effect of each of these variables on the coefficient of heat transfer after the authors presented their findings. An increase in Al_2O_3 concentration 1% or much less of the nanofluid's total mass was demonstrated to improve its heat transmission efficiency [12].

The purpose of this study was to evaluate the efficiency of heat transmission in a DPHE with a counterflow configuration using water with varying quantities of titanium carbid (TiC) and carbon nanotubes (CNT) nanoparticles. Nanofluid has been found to be more efficient than water at absorbing heat over a varied range of flow rates. The enhanced thermal properties of nanoscale fluids directly contribute to the increased efficiency of heat exchangers.

The rate at which heat is transferred is found to grow as the concentration of nanoparticles rises, according to additional studies.

Experimental set-up

Figure 1 depicts the double-pipe heat exchanger's (DPHE) defining characteristics. The sequential process is depicted graphically in fig. 2. The outer pipe is 80 mm in diameter, the inner pipe is 78 mm in diameter, and the total length of both pipes is 1.5 m. Both the outer and inner pipes are composed of copper, with the outer pipe measuring 60 mm in diameter and the inner pipe measuring 58 mm. The exterior of the pipe is insulated with a 45-millimeter-thick layer of mineral wool. Two separate manufacturers' SS 304 mono-block type centrifugal pumps are installed for piping hot and cold nanofluid, respectively. The cold nanofluid pump is on the right, while the hot water pump is on the left. The current temperature could be shown on the screen of a digital thermometer. In the first stage of testing, water is utilized in the heat exchangers to assess the effectiveness of the experimental set-up. Then, the system's CNT nanofluid and TiC nanofluid absorb and distribute the heat.

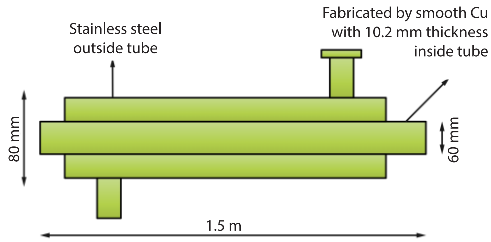

Figure 1. Specifications of twin pipe heat exchanger

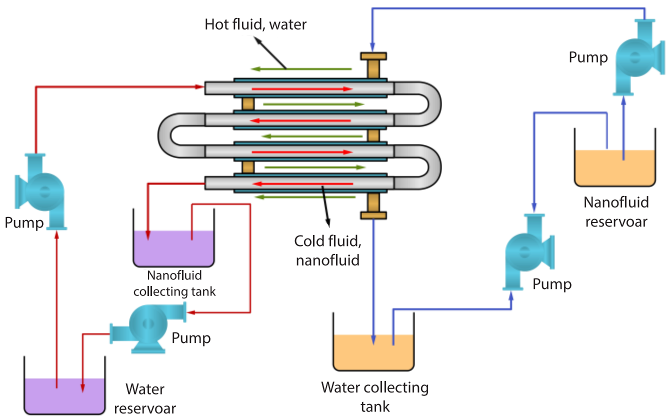

Figure 2. Systemic flow diagram of a counterflow DPHE

The overall coefficient of heat transfer of TiC and CNT nanofluid is obtained by measuring the input and output fluid temperatures. Both tanks need to be filled with water, but the first one should be hot and the second one cold. Chilling and distributing the nanofluid water from the exterior pipe should happen instantly. To measure the flow rate accurately, a rotameter should be utilized. Once the flow rates of the cold nanofluid and hot water have stabilized, the intake and output temperatures can be measured and recorded. The heat transfer rate can now be measured and analysed. Their responses to the varying nanofluid concentrations are subsequently measured as temperature changes. Once the tests are done, the tanks should be drained.

Nanofluid preparation

The most popular method for creating nanofluids is a two-stage procedure. Surfactants have a crucial role in increasing the nanoparticle's stability in solutions. One major challenge is ensuring that the surfactants can still perform as expected when subjected to high temperatures, as is often the case in certain types of applications. The underlying fluid and the TiC nanoparticles were mechanically stirred to ensure uniform mixing and distribution. Long-lasting solutions were formed by continuously agitating the nanofluid for around 34-46 juncture, according to the volume concentration being analysed. The TiC content was held constant at 0.03 wt.%, 0.06 wt.%, and 0.09 wt.% throughout the creation of the nanofluid, with the surfactant concentration ranging from 1-3. There were two-phases involved in making the CNT nanofluid. Dispersal of CNT nanoparticles in polar fluids such as water is facilitated by the ability of SDS molecules to *unzip* the nanoparticles. After that, CNT nanoparticles were introduced to the solution in an ultrasonicator bath. The frequency of the sonication of the ultrasonicator bath was held constant at 40 kHz. In some cases, the ultrasonicator bath temperature may rise above 45 °C. Following sonication, a dynamic condition was introduced to the CNT nanofluid by centrifuging it at 1800 rpm for 1 hour at regular intervals while maintaining CNT concentrations of 0.03 wt.%, 0.06 wt.%, and 0.09 wt.%. In addition, the initial sonication time of 70 minutes was doubled to a total of 190 minutes. Instructions for carrying out the steps depicted in fig. 3.

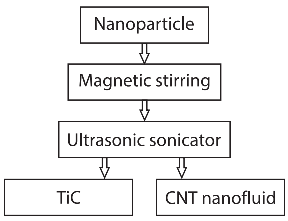

Figure 3. Nanofluid preparation

Determining the nanofluid's thermal conductivity early on is crucial for achieving a satisfactory level of agreement between theoretic predictions and real outcomes. The H-C pattern is utilised for predicting the thermophysical characteristics of nanofluids. The thermal conductivity of fluids is a commonpic of numerical research using this model [13, 14]:

$$k_{\mathrm{nf}} = \left[\frac{k_p + (m-1)k_t - (m-1)\varnothing(k_t - k_p)}{k_p + (m-1)k_t + \varnothing(k_t - k_p)} \right] k_t \tag{1}$$

It is possible to evaluate a particle's sphericity and the empirical form factor N based on its thermal conductivity if the particle is round. These properties characterize spherical particles. Table 1 displays the characteristics of the various nanofluids. Nanoparticles have a thermal conductivity denoted by the sign k_{nf}, while base fluids are represented by the symbol k_p. The thermal conductivity of nanoparticles is dramatically higher than that of more conventional fluids. The authors performed the following analysis to establish a model for the thermal conductivity of nanofluids [15]:

$$k_{\mathrm{nf}} = 0.25\left[(3\varnothing - 1)k_p + (2 - 3\varnothing)k_t\right] + \frac{k_t}{4}\sqrt{\Delta} \tag{2}$$

Table 1. Nanofluids properties

Nanofluid	Unit	TiC	CNT
Density	[kgm^{-3}]	3227	999
Specific heat	[JkgK^{-1}]	618	710
Thermal conductivity	[WmK^{-1}]	495	3511

Results and discussions

The thermal conductivity and fluid viscosity of TiC and CNT nanofluids

At 40 °C, as displayed in fig. 4, CNT thermal conductivity was greater than TiC. The CNT thermal conductivity was found to be optimally enhanced at a concentration of 0.09%. Figure 5 illustrates the impact of vol. concentration on the viscosity of a combination of TiC nanofluid and CNT at 40 °C. The CNT outperformed TiC nanofluid in terms of viscosity increase fluctuations at a working temperature of 40 °C. At a concentration of 0.03% by volume, both TiC and CNT saw increases in thermal conductivity of 28.21% and 32.14%, respectively.

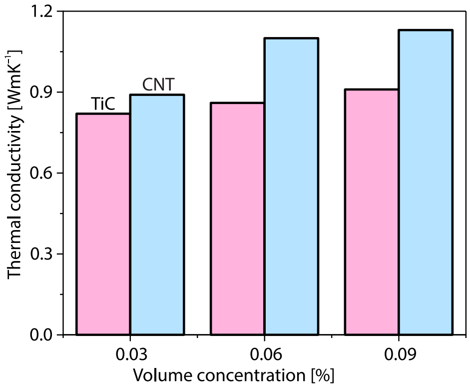

Figure 4. Thermal conductivity of TiC and CNT nanofluid

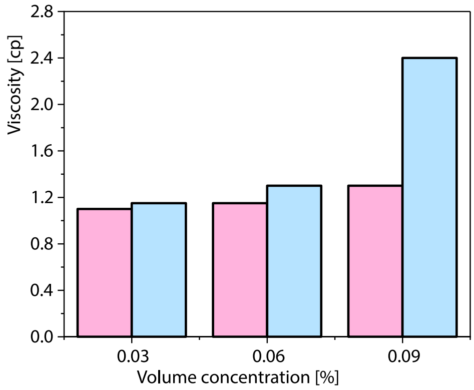

Figure 5. Viscosity of TiC and CNT nanofluid

Exploratory Nusselt number *vs*. linear correlation

The experimental Nusselt number of the TiC nanofluid was compared to that of the CNT, and correlations were discovered. The range of correlations found by various researchers was matched to volume concentrations found experimentally.

Coefficient of heat transfer and nusselt number for TiC and CNT nanofluids

Table 2 displays the improved thermal performance of the heat exchanger made possible by the employment of TiC nanofluid and CNT. This enhancement is a direct result of the efforts put in. Nusselt and Reynolds numbers are shown to be correlated in fig. 6(a) for TiC nanofluids and CNT. It was discovered that at a given flow rate, the Reynolds number of the TiC nanofluid was significantly smaller than that of the CNT nanofluid. The Nusselt number accurately predicts the projected rise in heat transfer rate. This is due to the fact that the dispersion of nanoparticles affects the thermal conductivity of the material. A comparison of the TiC nanofluid and CNT coefficients of transfer across all flow speeds is shown in fig. 6(b).

Table 2. The TiC and CNT have enhanced heat conductivity and viscosity

	Volume of concentration [%]	Elevated thermal conductivity [%]	Elevated viscosity [%]
TiC	0.03	31.33	15.8
	0.06	36.21	35.21
	0.09	38.96	32.51
CNT	0.03	32.37	17.9
	0.06	37.41	26.73
	0.09	41.31	34.56

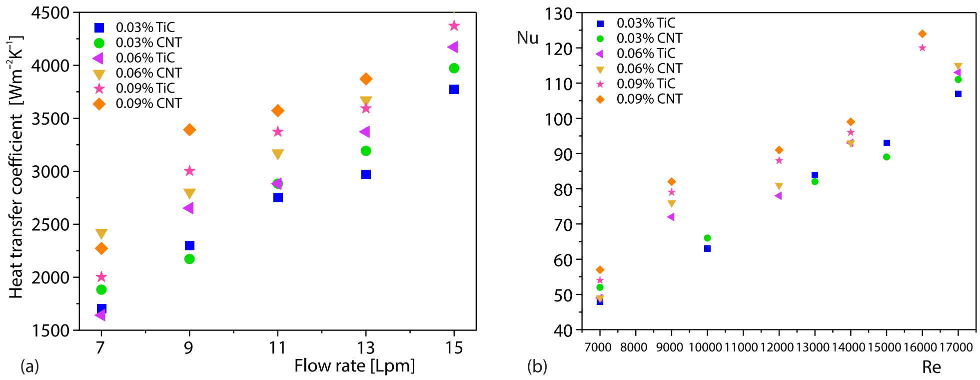

Figure 6. (a) Heat transfer coefficient and (b) Nusselt number during tests with the flow of TiC and CNT nanofluids

Analyzing the static pressure and drag coefficient of TiC and CNT nanofluids

Figure 7 (a) shows that as the Reynolds number was raised, the frictional coefficient decreased for both the TiC nanofluid and the CNT. The coefficient of friction of nanofluids was found to be essentially constant in all layers, even when the Reynolds number increased [14, 16]. It turned out to be like this. Figure 7(b) depicts the relationship between the pressure drop and the flow rate, which is a key indicator of the pumping power needed. The decrease in system pressure was directly proportional to the increase in TiC nanofluid and CNT particle concentration. Enhanced heat transmission and reduced pressure drop were given a numerical assessment by the thermal efficiency coefficient, which was calculated using eq. (3). This made it possible to identify the factor [17-19]:

$$\eta = \frac{\dfrac{\mathrm{Nu}_{\mathrm{nf}}}{\mathrm{Nu}_{\mathrm{bf}}}}{\left(\dfrac{f_{\mathrm{nf}}}{f_{\mathrm{bf}}}\right)^{1/3}} \tag{3}$$

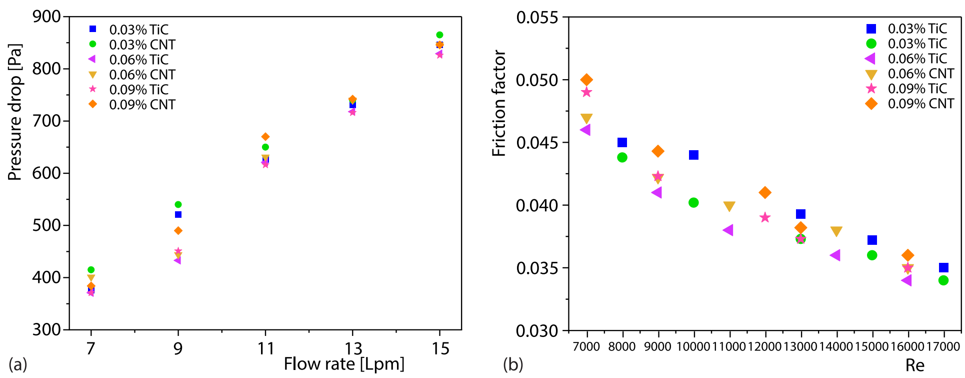

Figure 7. (a) Coefficient of friction using the Reynold's number and (b) flow rate using pressure dropsthe of TiC and CNT nanofluids

These findings suggest that TiC nanofluid combined with CNT produces a suitable working fluid. The CNT-containing TiC nanofluid performs brilliantly as a fluid for heat transfer even at concentrations as small as 0.03%.

Analyzing TiC and CNT nanofluids with CFD

Researchers are looking at the fluid-flow and heat transfer capabilities of TiC and CNT-based materials. Within the applicable geometry, buoyancy force drives nanofluid motion owing to the effect of natural-convection. The inner tube maintains a constant speed of 1 m/s while transporting TiC nanoparticles and CNT at an input temperature of 23 °C. Using an input temperature of 90 °C, fluid is pumped at a constant speed of 1 m/s through the outer tube. There is a noticeable cooling of the hot fluid upon introduction of the cold TiC nanofluid, resulting in a departure temperature of 72 °C. To the right of the pattern, the baking fluid is at a much lower temperature compared to the left. Figure 8 shows that when the output temperature is set to 43 °C, the temperature of the TiC nanofluid will rapidly increase.

Some enhancements have been made to the flow patterns of CNT. The TiC nanolow fluid's rate of spontaneous convection may be due to the fluid's high density. The fluid's density influences both its buoyancy and its speed. The TiC has a larger density than CNT, but its heat conductivity is much lower. The exit temperatures for CNT and hot fluid are 48 °C and 68 °C, respectively. When comparing the two geometries side by side, we can see that the pressure difference between the inside and outflow is greater in the CNT geometry. Variables such as fluid-flow speed, pipe surface friction, heat exchanger use frequency, density of the bulk, and viscosity all impact pressure differentials. Figure 8 shows the concentration dependence of the thermal performance factor for TiC nanofluid and CNT.

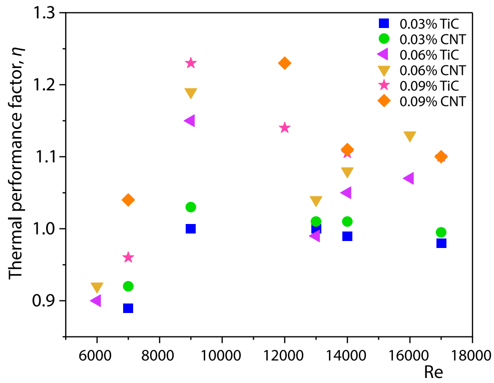

Figure 8. Thermal performance factors of the TiC and CNT nanofluids

Conclusions

Concentrate volumes as low as 0.03-0.06% were used in the experiments to examine the heat transmission and flow characteristics of the TiC and the CNT. Some possible conclusions from the research are as follows.

- Even at volume concentrations as low as 0.09%, the thermophysical factors of the TiC nanofluid and CNT are significantly improved.
- The CNT nanofluid showed higher heat fetch capabilities, as seen by a 68.2% increase in thermal efficiency compared to the 0.09% TiC nanofluid.
- At a Reynolds number of 9000, the highest thermal attainment element for 0.06% TiC was 1.26, while for CNT it was 2.84.
- The temperature and pressure along the contour are more uniform in CNT nanofluid than in TiC nanofluid because of CNT nanofluid's better thermal conductivity and lower density.

References

[1] Nematpour Keshteli, A., *et al.*, Thermal Enhancement Techniques for a Lobed-Double Pipe PCM Thermal Storage System, *Appl. Therm. Eng.*, *233* (2023), 121139

[2] Porgar, S., *et al*., Physiochemical Studies of Functionalized MWCNT/Transformer Oil Nanofluid Utilized in a Double Pipe Heat Exchanger, *Can J. Chem*., *99* (2021), 6, pp. 510-518
[3] Li, Z. X., *et al*., Nanofluids as Secondary Fluid in the Refrigeration System: Experimental Data, Regression, ANFIS, and NN modelling, *Int. J. Heat Mass Transf*., *144* (2019), 118635
[4] Alsarraf, J., *et al*., Hydrothermal Analysis of Turbulent Boehmite Alumina Nanofluid-Flow with Different Nanoparticle Shapes in a Minichannel Heat Exchanger Using Two-Phase Mixture Model, *Physica A: Statistical Mechanics and its Applications*, *520* (2019), Apr., pp. 275-288
[5] Hashemi Karouei, S. H., *et al*., Laminar Heat Transfer and Fluid-Flow of Two Various Hybrid Nanofluids in a Helical Double-Pipe Heat Exchanger Equipped with an Innovative Curved Conical Turbulator, *J ournal Therm. Anal Calorim.*, *143* (2021), 2, pp. 1455-1466
[6] Saleh, B., Syam Sundar, L., Thermal Performance, Embodied Energy and Environmental CO_2 Emissions Analyses for Double Pipe U-Bend Heat Exchanger Working with MWCNT/water Nanofluid, *International Journal of Thermal Sciences*, *169* (2021), 107094
[7] Monfared, M., *et al*., Second Law Analysis of Turbulent Convection Flow of Boehmite Alumina Nanofluid Inside a Double-Pipe Heat Exchanger Considering Various Shapes for Nanoparticle, *Journal Therm. Anal. Calorim*., *135* (2019), 2, pp. 1521-1532
[8] Ali, F. A., *et al*., The Impact of Alumina Nanoparticles Suspended in Ethylene Glycol on the Performance Efficiency of a Double Pipe Heat Exchanger, *Frontiers in Heat and Mass Transfer*, *15* (2020), 21, pp. 1-7
[9] Khakpour, M., Vaferi, B., Experimental and Modelling Analyses of Stability and Thermophysical Characteristics of Graphene Oxide, Carbon Nanotube, and Silicon Carbide Dispersion in Propylene Glycol, *Heat Transf. Res*., *54* (2023), 14, pp. 1-15
[10] Abu-Hamdeh, N. H., *et al*., Improve the Rheological and Thermal Performances of the Antifreeze Liquids for Cooling the Batteries and Radiators in Automobiles Via Provide a New Hybrid Material Composed from Carbon Nanotubes in Ethylene Glycol/Propylene Glycol, *Journal Energy Storage*, *52* (2022), 104982
[11] Kasaeipoor, A., *et al*., Free Convection Heat Transfer and Entropy Generation Analysis of MWCNT-MgO (15-85%)/Water Nanofluid Using Lattice Boltzmann Method in Cavity with Refrigerant Solid Body-Experimental Thermo-Physical Properties, *Powder Technol.*, *322* (2017), Dec., pp. 9-23
[12] Mithran, R., Sadhasivam, C., Experimental Studies of Pressure Drop in Compact Heat Exchanger with Aluminum Oxide and Magnesium Oxide, *International Journal of Mechanical and Production Engineering Research and Development*, *9* (2019), 6, pp. 525-534
[13] Ramesh, B., *et al.*, Optimization and Experimental Analysis of Drilling Process Parameters in Radial Drilling Machine for Glass Fiber/Nanogranite Particle Reinforced Epoxy Composites, *Mater Today Proc*., *62* (2022), Part 2, pp. 835-840
[14] Girimurugan, R., *et al*., Static and Total Pressure Analysis of Three Way Catalytic Convertor Using CFD, *107* (2022), 1, pp. 7381-7387
[15] Khetibet Y., *et al*., The Influence of Forced Convective Heat Transfer on Hybrid Nanofluid-flow in a Heat Exchanger with Elliptical Corrugated Tubes: Numerical Analyses and Optimization, *Applied Sciences (Switzerland)*, *12* (2022), 6, 2780
[16] Sangeetha, A., *et al*., Experimental Evaluation and Thermodynamic Gibbs Free Energy Analysis of a Double-Slope U-Shaped Stepped Basin Solar Still Using Activated Carbon with ZnO Nanoparticles, *Journal Clean Prod*., *380* (2022), 135118
[17] Girimurugan, R., *et al.*, Application of Deep Learning to the Prediction of Solar Irradiance through Missing Data, *International Journal of Photoenergy*, *2023* (2023), ID4717110
[18] Gift, M. D. M., *et al*., Determination of Prohibition Mechanism of Cationic Polymer/SiO_2 Composite as Inhibitor in Water Using Drilling Fluid, *Mater Today Proc*., *69* (2022), Part 3, pp. 1080-1086
[19] Murugan, M., *et al*., Enhancing Productivity of V-trough Solar Water Heater Incorporated Flat Plate Wick-Type Solar Water Distillation System, *Journal Heat Transfer*, *143* (2021), 3, 032001

Paper submitted: March 12, 2023
Paper revised: September 16, 2023
Paper accepted: October 21, 2023